Micro and Nano Engineering 9 (2020) 100076

Contents lists available at ScienceDirect

Micro and Nano Engineering

journal homepage: www.journals.elsevier.com/micro-and-nano-engineering

Research paper

# High sensitive refractive index sensor based on spatial symmetry breaking Fano metamaterials fabricated by ion beam irradiation

Shuo Du[a,b], Zhe Liu[c], Haifang Yang[a], Junjie Li[a,d], Changzhi Gu[a,b,*]

[a] Beijing National Laboratory for Condensed Matter Physics, Institute of Physics, Chinese Academy of Sciences, Beijing 100190, China
[b] School of Physical Sciences, CAS Key Laboratory of Vacuum Physics, University of Chinese Academy of Sciences, Beijing 100049, China
[c] Niels Bohr Institute, University of Copenhagen, Blegdamsvej 17, DK-2100 Copenhagen, Denmark
[d] Songshan Lake Materials Laboratory, Dongguan, Guangdong 523808, China

A B S T R A C T

The sensitivity of plasmonic nanostructures based refractive index sensor can be improved by free-standing three-dimensional (3D) configuration. Here, by means of focused-ion-beam (FIB) induced folding technique, we fabricated arbitrary spatially oriented double-flake 3D metamaterials (MMs). The experimental measured sensitivity can reach 2703 nm/RIU, and based on the symmetry breaking configuration, the figure of merit (FoM) reaches 37.2 $RIU^{-1}$ in simulation results. What's more, the different coupling mechanisms in our MMs enable the independent modulation of each resonance. This work opens up new avenues for near-field coupling modulation, holding great potential applications in multi-resonance differential sensing, switch devices and optical communication.

## 1. Introduction

Metamaterials (MMs), composite artificial materials structured on the subwavelength scale, are powerful means for wave manipulation [1–3]. Plasmonic nanostructures are one of the most common elements to construct MMs, and many fascinating optical properties have been explored based on them [1,4–8]. Optical sensor for refractive index measurement has long been a promising application for plasmonic MMs, due to most of their resonances are largely affected by the refractive index variation. In order to characterize the sensing performance, two important criteria, sensitivity and figure of merit (FoM), are used [9]. The refractive index sensitivity refers to the ratio of the change in resonant wavelength caused by refractive index variation, and the FoM normalizes the sensitivity to the width of resonance curve. Numerous attempts have been made to enhence them, and obtaining a resonance with sharp spectral line-shape is an efficient approach [10–13]. Fano resonance, generated by the interference between a narrow discrete state and a broad continuum state, has an asymmetric and steep spectral line-shape [14,15], which is very useful to enhance the FoM. Conventional method for Fano-type MMs is adopting symmetry breaking structures in unit design [16–18], e.g. asymmetrically split-ring resonators (ASRs) [16,17], which brings access to the asymmetric line-shape resonances with narrow curve width. However, it is hard to get a satisfactory sensitivity, because most of the Fano MMs are two-dimensional configuration, thus the resonators can't be fully exposed to the environment, which limits the effects of the refractive index variation on the resonance. Recently, focused-ion-beam (FIB) irradiation induced folding technique can provide us with solutions. By it, the fabricated three-dimensional (3D) MMs can be implemented. The vertical free-standing split ring resonators (SRR) and metallic holes (MHs) composite MM can provide the out-of-plane near field couplings [19,20], and the generated Fano resonance offers a high sensitivity approaching 2040 nm/RIU [19]. In fact, the folding angle of the FIB induced folding technique is the flexible, so that the spatially oriented nano-resonators can be easily implemented [21]. However, most of the designed units in related works only focused on vertical 3D construction, while the flexibility in orientation modulation is underutilized.

In this work, the FIB induced folding technique is used to design and fabricate arbitrary spatially oriented double-flake 3D MMs. By tuning the angle of inclination, the symmetry of structure unit can be broken, resulting in a new Fano resonance at lower frequency. The sensitivity of the new resonance can reach 2703 nm/RIU and FoM 24.5 $RIU^{-1}$ by measurement. Besides, the coupling mechanisms of these two Fano resonances are completely different, which gives the possibility to independently modulate each resonance. The distance variation between two flakes results in a much significant change of peak width for the resonance at high frequency than that at low frequency. On the contrary, by changing the width of flakes, the resonance at higher frequency remains unchanged, while the sensitivity of the one at lower frequency is modulated from 1600 nm/RIU to 2703 nm/RIU in near-infrared region. Our work enriches the approach of near-field coupling modulation and is promising in applications such as optical switches and differential multi-resonance sensing.

* Corresponding author.
*E-mail address:* czgu@iphy.ac.cn (C. Gu).

https://doi.org/10.1016/j.mne.2020.100076
Received 17 November 2019; Received in revised form 28 May 2020; Accepted 17 September 2020

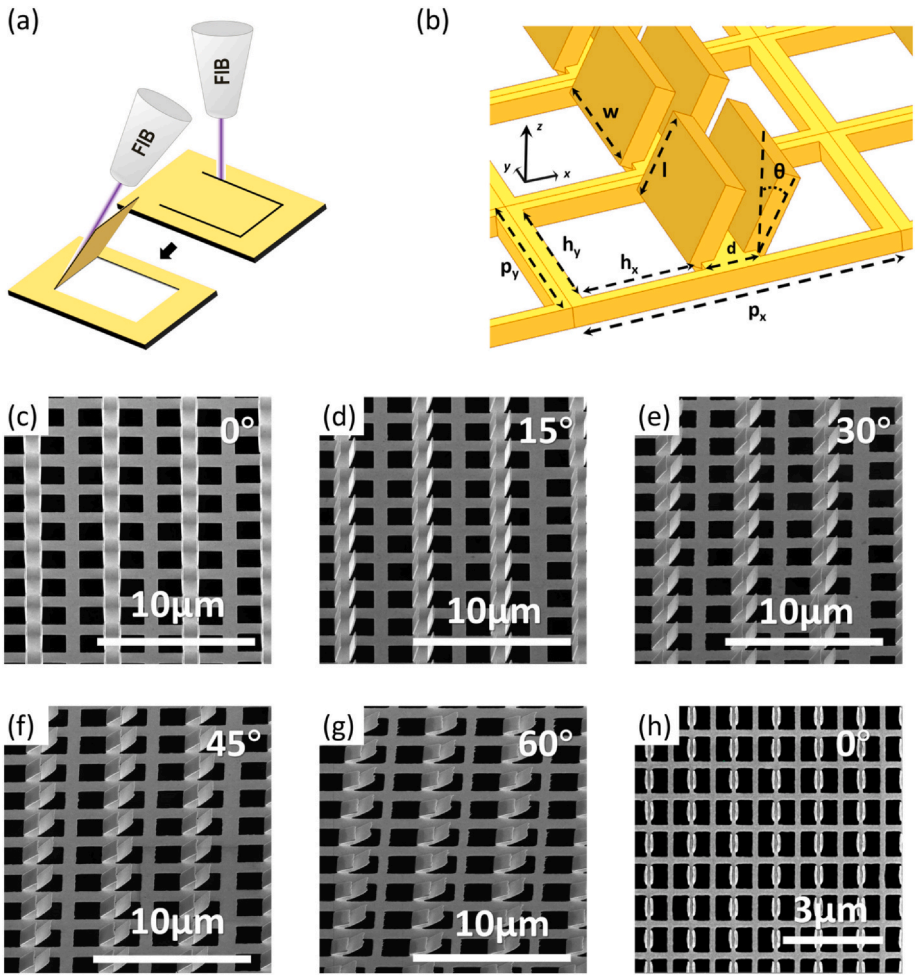


**Fig. 1.** (a) Illustration of main steps of FIB folding technique. (b) Schematic of double-flake MMs. (c) to (g) SEM images of flakes with folding angle varying from 0° to 60°. (h) Double-flake MM that operates in near-infrared region.

### *1.1. Material and method*

The schematic of main fabrication steps is shown in Fig. 1(a). First, an FIB system (FEI Helios 600i) is used for ion-beam nano-patterning on the self-supporting gold film with a thickness of 60 nm. This film was deposited on a 1.2 μm layer of S1813 photoresist and then suspended in acetone when the resist is dissolved. A transmission electron microscope copper grid was used to pick up the released gold film from the solution [19]. The pre-designed sophisticated patterns are firstly etched by ion-beam to get suspended gold flakes. Next, the ion-beam direction is readjusted to a specific angle to irradiate on the root of the flakes, which makes the flakes fold towards the direction of ion-beam. The acceleration voltage of $Ga^+$ was 30 kV. An ion-beam current of 40 pA was used for the present work.

Fig. 1(b) is the schematic diagram of spatial-symmetry-breaking Fano MM, which consists of double flakes and MHs. Fig. 1(c)–(g) are the SEM images of flakes with folding angles varying from 0° to 60°, and the fabricated samples are of high homogeneity in large area. Fig. 1(h) shows the MM that is scaled down and operates in near-infrared region. The width (w) and length (l) of the flake are chosen as w = 600 nm and l = 300 nm. The distance between two flakes (d) is chosen as d = 200 nm. Other parameters are chosen as $h_x$ = 450 nm, $h_y$ = 700 nm, $p_x$ = 1200 nm, $p_y$ = 800 nm and the folding angle θ is chosen to be 0° and 30°. The transmission spectra of the scaled-down MMs were simulated by finite-difference time-domain (FDTD) method, and measured by Fourier-transform infrared spectrometer.

## 2. Results and discussion

The MMs are illuminated by x-polarized light and the transmission spectra are shown in Fig. 2. When θ = 0°, there's only one resonance in Fig. 2(a) at 1.63 μm (mode *I*), which shows an asymmetric feature of Fano resonance. As θ switches from 0° to 30°, a similar resonance (mode *II*) remains at this position while a new resonance (mode *III*) appears at around 2.7 μm which can be seen in Fig. 2(c), by symmetry breaking of the structure in x direction. Compared with mode *I* (1.63 μm) and *II* (1.52 μm), mode *III* has a narrower line-shape but lower modulation depth (the difference between the maximum and minimum value of the resonance). When the refractive index of environment changes from 1 to 1.36, the sensitivity (calculated by S = Δλ/Δn) of mode *III* is 2417 nm/RIU, which is much higher than mode *I* (1611 nm/RIU) and *II* (1492 nm/RIU). Besides, the FoM value of mode *III* is 37.2 $RIU^{-1}$, which is nearly five-fold of mode *I* (8.1 $RIU^{-1}$) and *II* (7.5 $RIU^{-1}$). The results of experimental measurement in Fig. 2(b) and 2(d) show that, the double-flake MM at θ = 30° does bring a new resonance mode, which exhibits a higher sensing sensitivity of 2703 nm/RIU and a larger FoM of 24.5 $RIU^{-1}$ compared to mode *I* and *II*. The measured results basically consistent with the results of the simulations, where the slight differences in the resonant wavelength and resonant strength primarily arises from imperfections in the fabrication process.

To reveal the underlying mechanism of resonances, the surface current distributions of these three modes are presented by the commercial software CST Microwave Studio. As illustrated in Fig. 3 (a), the circulating currents inside the two flakes have contributed most to

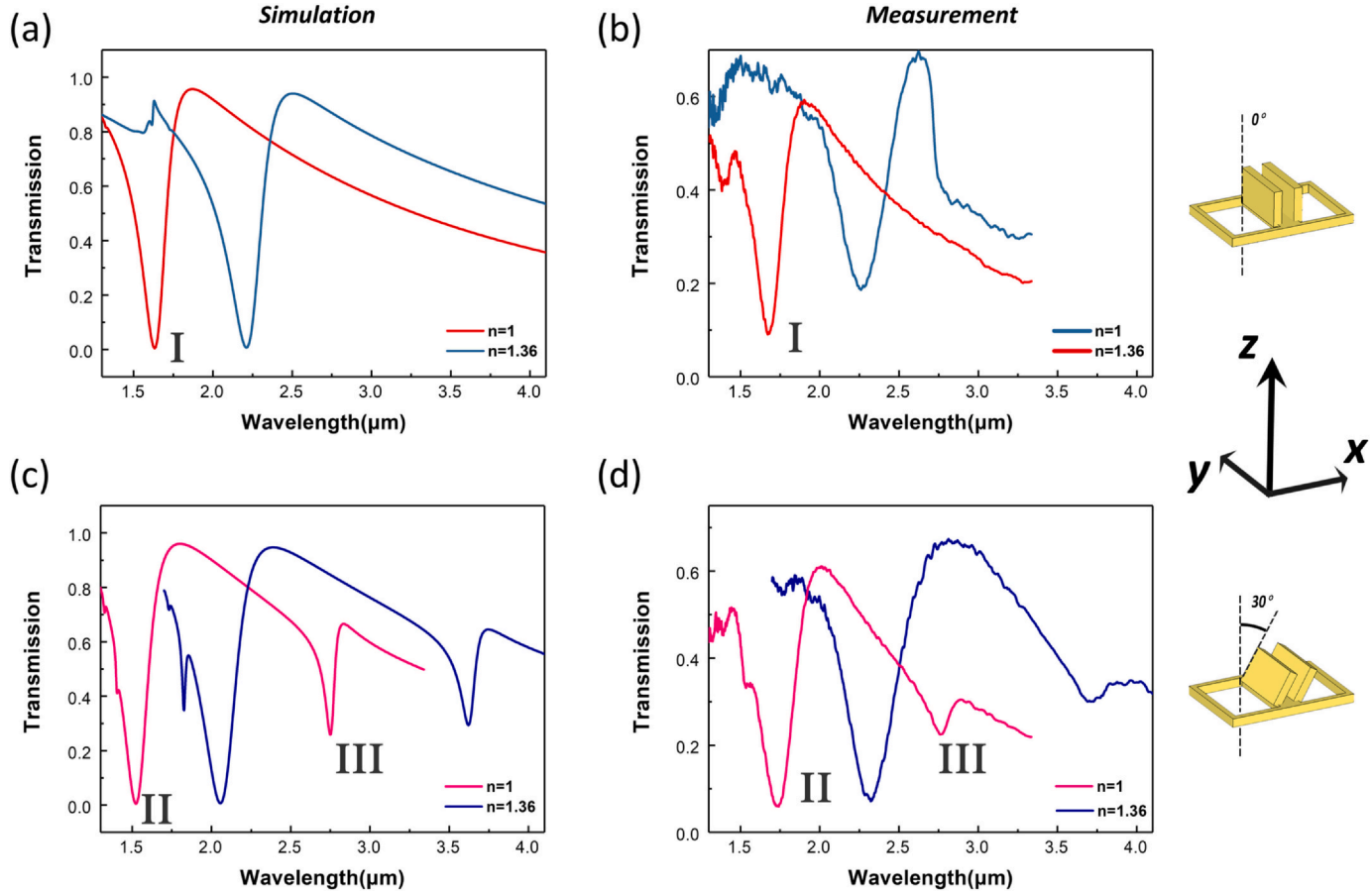


**Fig. 2.** Simulated and experimental transmission spectra of double-flake MMs in the environment with refractive indices of 1 and 1.36 respectively. (a) and (b) Spectra of MMs folded to 0°. (c) and (d) Spectra of MMs folded to30°.

mode *I* which is a magnetic response excited by y-component of magnetic field, and the currents on the edges of periodic MHs from surface plasmon polaritons (SPPs) are relatively weak. When the flakes are tilted to 30°, mode *II* has almost the same current distribution (Fig. 3(a) *II*) and wavelength compared to mode *I* while a new resonance mode *III* appears, with hardly any current circulation inside the flakes (Fig. 3(a) *III*). Instead, currents can be found on the edges of MHs and outside of flakes. The currents on MHs comes again from SPPs, while the $E_z$ components of SPPs contribute to current on the outside surfaces of flakes (i.e., localized surface plasmon (LSP)), and the coupling between SPPs and LSP contribute to this new resonance [20]. To clearly illustrate the transition among the three modes, a colormap of simulated transmission spectra versus the folding angle are shown in Fig. 3(b). When $\theta = 0°$, only mode *I* can be found in the spectrum, while mode *III* is hidden due to the symmetric configuration. As the angle increases, mode *III* appears immediately, with the modulation depth becomes deeper and the peak width goes larger, which results in a decrease of FoM. Therefore, the folding angle should be appropriately chosen to meet the trade-off between modulation depth and FoM.

To further demonstrate the difference between mode *I/II* and mode *III*, the two elements for optical coupling of each mode are separately studied. For mode *I* and *II*, the 3D MM is divided into two parts, U-shaped double flakes (the bottom part of the U-shape is included to introduce the circular current) and MHs, as shown in the inset of Fig. 4(a). The red curve (magnetic response on U-shaped double flakes) in Fig. 4(a) has a symmetric line-shape, which can serve as a discrete resonance state, while the blue curve coming from the extraordinary optical transmission (EOT) [20] of MHs serves as a continuum state. When the two parts are combined together, the near-field coupling results in the Fano resonance which can be seen from the yellow curve. It should be emphasized that the two states are independent with each other, which has a different coupling mechanism compared to mode *III*.

For mode *III*, the resonance is generated from the coupling between the near-field of surface currents on the outside of flakes from LSP and MHs from SPP. As discussed above, the LSP is excited by evanescent wave from SPP instead of incident light. In this case, the LSP intensity is highly depended on the near-field coupling strength. This can be proved by the simulation result in Fig. 4(b) where the double flakes are lifted up from MHs with different heights (the distance from the top-surface of MHs to the bottom of the flakes, picked as 0, 50, 90, and 190 nm). There's a prominent resonance when the two parts are connected (0 nm height), but as the height increases, the resonance intensity reduces rapidly due to the fast attenuation of evanesce wave. This indicates a different coupling scheme of mode *III* that the two states of Fano resonance are highly correlated.

Due to the different coupling mechanisms between mode *II* and *III*, the behavior of each resonance can be modulated independently. As shown in Fig. 5(a), by increasing the distance d between two flakes, the resonance linewidth of mode *II* broadens, but it has a minor effect on mode *III*. That's because d is a key parameter of the U-shape resonator of mode *II*, but for mode *III* the currents concentrate on the MH edges and the outside of the flakes which has limited relation to distance d. Similarly, mode *III* can be modulated independently through flake width w, as shown in Fig. 5(b). When w varies from 100 nm to 600 nm, the resonance wavelength of mode *III* red-shifts from 1.72 μm to 2.75 μm, while mode *II* remains unchanged. That is because the surface currents of mode *III* partially move diagonally on the flakes (in Fig. 3(a) *III*), thus the increasing w effectively elongates the LSP route. But for mode *II*, the flake width has nothing to do with the perimeter of U-shaped current loop from magnetic response in the x-z plane. When

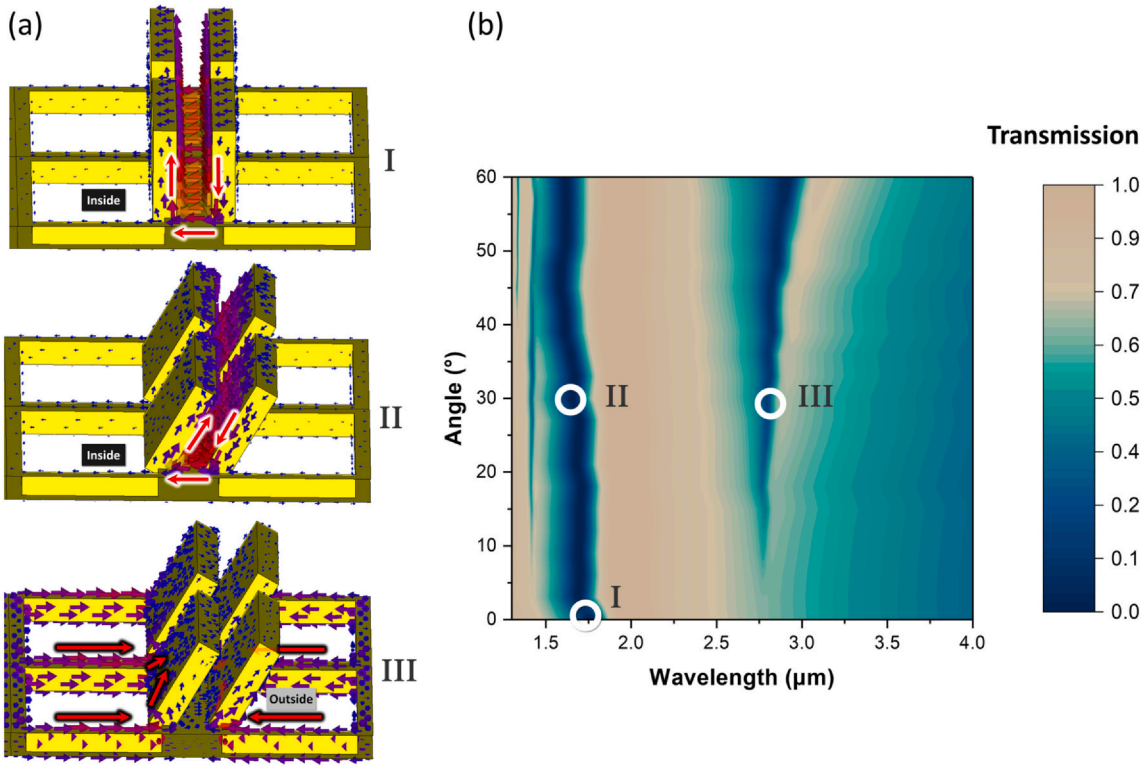


**Fig. 3.** (a) Surface current distribution of mode *I*, *II* and *III*. (b) Colormap of the simulated transmission spectra versus the folding angle. The mode *I*, *II* and *III* are marked by white circles.

length l and distance d is fixed, mode *II* stays unchanged. What's more, the sensing sensitivity of mode *III* can also be modulated in this process, as shown in Fig. 5(c), that when the flakes broaden, the sensitivity difference between mode *II* and mode *III* increases rapidly, which could be used to implementing multi-resonances differential sensing.

## 3. Conclusion

In summary, by means of FIB folding technique, we have designed and implemented an arbitrary spatially oriented double-flake 3D MMs. The near-field coupling between double flakes and MHs generates obvious Fano resonance in near-infrared region. The 3D self-standing configuration enables the high sensitivity of Fano resonance for refractive index sensing. By further breaking the structure symmetry, a new resonance with a very high sensitivity of 2703 nm/RIU and FoM of 24.5 $RIU^{-1}$ has been observed. What's more, the behavior of each resonance can be modulated independently. This work provides new prospects for near-field coupling modulation, holding potential applications in multi-resonances differential sensing, switch devices, color displays and optical communication.

## Declaration of Competing Interest

We would like to submit the enclosed manuscript entitled “High sensitive refractive index sensor based on spatial symmetry breaking Fano metamaterials fabricated by ion beam irradiation”, which we wish to be considered for publication in “Micro and Nano Engineering”. No

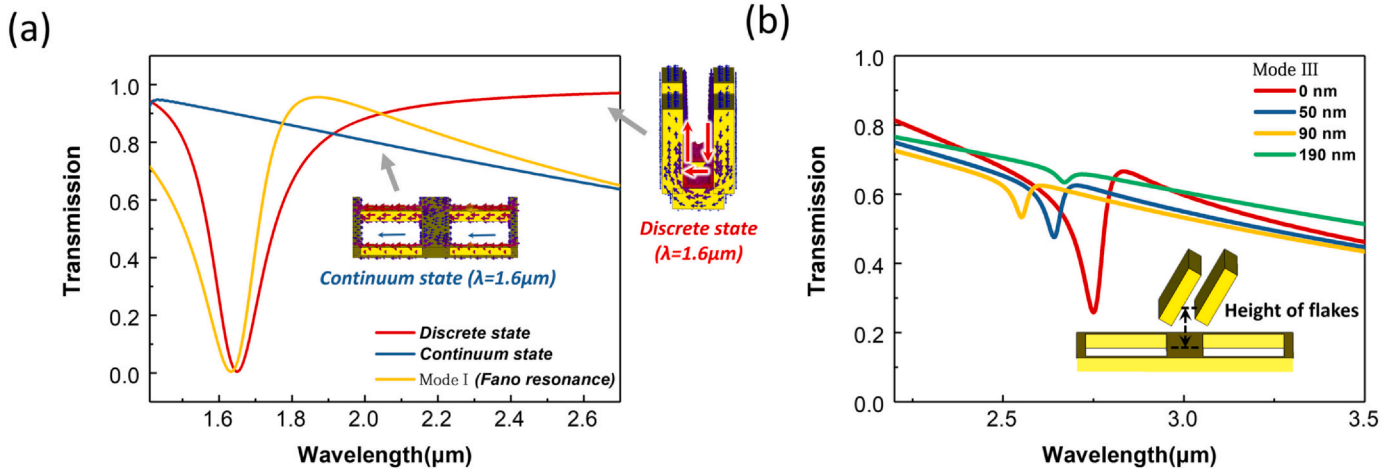


**Fig. 4.** (a)Simulated transmission spectra and surface current distribution of double flakes (discrete state) and MHs (continuum state). (b) Simulated transmission spectra of MHs with lifted double flakes with different distance.

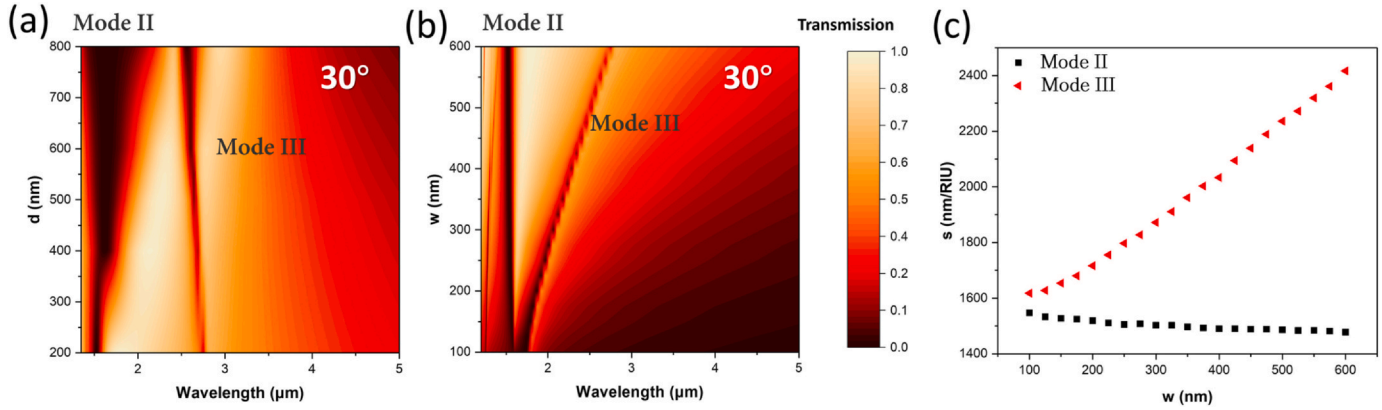


**Fig. 5.** Colormap of simulated transmission spectra of the proposed structure with folding angle of 30° versus the distance d between flakes (a) and flake width w (b). (c) The sensitivity of mode *II* and *III* as a function of flake width w.

conflict of interest exists in the submission of this manuscript, and the manuscript is approved by all authors for publication.

## Acknowledgements

This work was supported by the National Key Research and Development Program of China (Grant Nos. 2016YFA0200400, and 2016YFA0200800), National Natural Science Foundation of China (Grant Nos. 91323304, 11674387, 11504414, 11574369, 11574385, 11574369, 61390503), Strategic Priority Research Program of the Chinese Academy of Sciences (Grant No. XDB07020200) and Key Research Program of Frontier Sciences, CAS (Grant No. QYZDJ-SSW-SLH042).

## References

[1] D. Schurig, J.J. Mock, B.J. Justice, B.J. Justice, S.A. Cummer, J.B. Pendry, A.F. Starr, D.R. Smith, Metamaterial electromagnetic cloak at microwave frequencies, Science 314 (2006) 977–980.
[2] J.K. Gansel, M. Thiel, M.S. Rill, M. Decker, K. Bade, V. Saile, G. von Freymann, S. Linden, M. Wegener, Gold helix photonic metamaterial as broadband circular polarizer, Science 325 (5947) (2009) 1513–1515.
[3] W.J. Padilla, A.J. Taylor, C. Highstrete, M. Lee, R.D. Averitt, Dynamical electric and magnetic metamaterial response at terahertz frequencies, Phys. Rev. Lett. 96 (10) (2006) 107401.
[4] M.K. Hedayati, M. Elbahri, Review of metasurface plasmonic structural color, Plasmonics 12 (5) (2017) 1463–1479.
[5] M.I. Stockman, Nanoplasmonics: past, present, and glimpse into future, Opt. Express 19 (22) (2011) 22029–22106.
[6] A. Pors, S.I. Bozhevolnyi, Plasmonic metasurfaces for efficient phase control in reflection, Opt. Express 21 (22) (2013) 27438–27451.
[7] F. Monticone, A. Alu, Metamaterial, plasmonic and nanophotonic devices, Rep. Prog. Phys. 80 (3) (2017) 37.
[8] M. Iwanaga, Photonic metamaterials: a new class of materials for manipulating light waves, Sci. Technol. Adv. Mater. 13 (5) (2012).
[9] Y. Xu, P. Bai, X. Zhou, Y. Akimov, C.E. Png, L.K. Ang, W. Knoll, L. Wu, Optical refractive index sensors with plasmonic and photonic structures: promising and inconvenient truth, Adv. Opt. Mater. 7 (9) (2019) 1801433.
[10] A.B. Khanikaev, C.H. Wu, G. Shvets, Fano-resonant metamaterials and their applications, Nanophotonics 2 (4) (2013) 247–264.
[11] B. Gallinet, O.J.F. Martin, Refractive index sensing with subradiant modes: a framework to reduce losses in Plasmonic nanostructures, ACS Nano 7 (8) (2013) 6978–6987.
[12] L.V. Brown, H. Sobhani, J.B. Lassiter, P. Nordlander, N.J. Halas, Heterodimers: plasmonic properties of mismatched nanoparticle pairs, ACS Nano 4 (2) (2010) 819–832.
[13] J. Zhao, C. Zhang, P.V. Braun, H. Giessen, Large-area low-cost plasmonic nanostructures in the NIR for fano resonant sensing, Adv. Mater. 24 (35) (2012) OP247–OP252.
[14] M.F. Limonov, M.V. Rybin, A.N. Poddubny, Y.S. Kivshar, Fano resonances in photonics, Nat. Photonics 11 (9) (2017) 543–554.
[15] A.E. Miroshnichenko, S. Flach, Y.S. Kivshar, Fano resonances in nanoscale structures, Rev. Mod. Phys. 82 (3) (2010) 2257–2298.
[16] V.A. Fedotov, M. Rose, S.L. Prosvirnin, N. Papasimakis, N.I. Zheludev, Sharp trapped-mode resonances in planar metamaterials with a broken structural symmetry, Phys. Rev. Lett. 99 (14) (2007).
[17] K. Aydin, I.M. Pryce, H.A. Atwater, Symmetry breaking and strong coupling in planar optical metamaterials, Opt. Express 18 (13) (2010) 13407–13417.
[18] F. Hao, Y. Sonnefraud, P. Van Dorpe, S.A. Maier, N.J. Halas, P. Nordlander, Symmetry breaking in plasmonic nanocavities: subradiant LSPR sensing and a tunable Fano resonance, Nano Lett. 8 (11) (2008) 3983–3988.
[19] A. Cui, Z. Liu, J. Li, T.H. Shen, X. Xia, Z. Li, Z. Gong, H. Li, B. Wang, J. Li, H. Yang, W. Li, C. Gu, Directly patterned substrate-free plasmonic "nanograter" structures with unusual Fano resonances, Light-Sci. Appl. 4 (2015).
[20] Z. Liu, Z. Liu, J. Li, W. Li, J. Li, C. Gu, Z.Y. Li, 3D conductive coupling for efficient generation of prominent Fano resonances in metamaterials, Sci. Rep. 6 (2016) 27817.
[21] Z. Liu, A. Cui, Z. Gong, H. Li, X. Xia, T.H. Shen, J. Li, H. Yang, W. Li, C. Gu, Spatially oriented plasmonic 'nanograter' structures, Sci. Rep. 6 (1) (2016).